

Atomic structures and energetics of LaNi₅-H solid solution and hydrides

Kazuyoshi Tatsumi,* Isao Tanaka, Haruyuki Inui, Katsushi Tanaka, Masaharu Yamaguchi, and Hirohiko Adachi
Department of Materials Science and Engineering, Kyoto University, Sakyo, Kyoto 606-8501, Japan
 (Received 15 March 2001; revised manuscript received 29 May 2001; published 18 October 2001)

First-principles calculations on a primary solid solution of LaNi₅-H and a hypothetically ordered full hydride, LaNi₅H₇ have been made employing ultrasoft pseudopotentials and plane-wave basis. Some intermediate hydrides were calculated as well. A full geometry optimization has been made to investigate their heat of formation in detail. Atomic positions of LaNi₅H₇ have been described in various ways through the Rietveld analyses of neutron-diffraction profile. The lowest energy structure by the present calculation is close to that of the model analyzed with the space group of $P6_3mc$ by Lartigue *et al.* However, we found that the structure model with a single unit cell, i.e., $Z = 1$, cannot be ruled out for LaNi₅H₇. Regarding the primary solid solution, the 12n site of LaNi₅ is most stable among five possible interstices proposed in literature. The stability of the interstices can be explained by the number of near-neighbor Ni atoms, which is substantially different from the widely accepted view that the geometric radius by the rigid sphere model determines the stability. The theoretical heat of solution in the primary solid solution is -33 kJ/mol-H₂, which roughly agrees with the experimental value. On the other hand, the heat of formation of LaNi₅H₇ is -45 kJ/mol-H₂, which is 30–40 % more negative than the experimental value. This discrepancy may be ascribed to the fact that all hydride samples are generally highly defective. The theoretical heat of formation of intermediate phases indicates that the LaNi₅-H system dissociates to the primary solid solution and the full hydride. Expansion of the cell volume associated with hydrogenation is well reproduced by the calculation.

DOI: 10.1103/PhysRevB.64.184105

PACS number(s): 61.50.Ah, 81.05.Bx, 81.05.Je

I. INTRODUCTION

LaNi₅ and its alloys are technologically very important since they show hydrogen-storage characteristics suitable for a wide range of applications including negative-electrode materials for rechargeable Ni-metal hydride (Ni-MH) batteries, hydrogen source for fuel cells, and energy-conversion/storage systems.^{1–3} In order to design the materials from macroscopic and/or microscopic scale, accurate knowledge of fundamental properties is essential. Although there have been a number of experimental works devoted to investigate the properties, the information is far from complete. Crystallographic studies of deuterated materials by neutron-powder diffraction have been repeatedly made. However, even a recent careful study was not able to determine unambiguously the structure of the LaNi₅H_{6.7}.⁴ Many studies on thermodynamic properties of the LaNi₅-H system have thus far been made. However, samples used in these studies were generally highly defective. For example, dislocation density of full hydride samples was reported to be in the order of 10^{15} m⁻².^{5–8} High concentration of vacancies was detected by positron annihilation study.⁹ However, no trial to distinguish the energy associated with the defects and real heat of hydrogenation has been made.

The electronic structure of the LaNi₅-H system has been investigated by a few groups. Experimental x-ray photoemission spectrum of H²⁺-implanted LaNi₅ was reported by Züchner *et al.*¹⁰ First-principles augmented plane wave (APW) calculation of LaNi₅ was first reported by Malik, Arlinghaus, and Wallace.¹¹ Gupta employed a semiempirical tight-binding method to qualitatively describe the electronic structure of LaNi₅ and LaNi₅H₇.¹² First-principles calculations using cluster models have been made to discuss the chemical bonding around hydrogen atoms.^{13,14} Recently,

first-principles band-structure calculations by linear combination of muffin-tin-orbital atomic-sphere-approximation (LMTO-ASA) method have been reported by three groups.^{15–17} Nakamura, Nguyen-Manh, and Pettifor¹⁵ discussed the energetics of hydrogen in the primary solid solution and the LaNi₅H₇ hydride. However, they used lattice parameters obtained from experiments and/or simplified geometric models. No relaxation around hydrogen atoms was taken into account. In summary, information provided by these electronic-structure investigations is only qualitative despite these efforts. Quantitatively reliable theoretical calculations to elucidate the atomic positions of hydrides and evaluate the energies of the hydrogenation have, therefore, been strongly desired. Once the structure is determined, further theoretical calculations of various properties can be made in a straightforward manner. This information should be very useful for the analysis of the experimental spectra as well.

In the present study, we adopt a first-principle approach having quantitative reliability and sufficient predictive power. A plane-wave basis pseudopotential (PW-PP) method is chosen because of its efficiency and accuracy in geometry optimization of complex systems with many degrees of freedom. Atomic positions are carefully examined after the full optimization of the structure. The theoretical structures and lattice parameters are compared with models proposed by experiments. Heats of formation and/or solution are then computed to compare with the experimental values when they are available.

II. COMPUTATIONAL PROCEDURES

The calculations presented in this work were performed within the generalized-gradient approximation¹⁸(GGA) to

density-functional theory, using a PW-PP method.¹⁹ The density mixing scheme by Kresse and Furthmüller²⁰ was used to obtain the Kohn-Sham ground state in conjunction with the conjugate-gradient algorithm.²¹ Atomic positions were optimized using quasi-Newton method with Broyden-Fletcher-Goldfarb-Shanno hessian-update scheme.²² In order to reduce the size of the number of the plane-wave basis set, ultrasoft pseudopotentials²³ were employed. The pseudopotentials were constructed for neutral atoms. The La-4*f* orbital was therefore not included. It has been demonstrated that the ultrasoft potentials provide great improvements in both accuracy and computational costs for elements with the valence 1*s*, 2*p*, 3*d*, or 4*f* electrons where the norm-conserving potentials are necessarily quite hard.²⁴ In the present study, we need to calculate H and Ni in which 1*s* and 3*d* electrons play major roles in the electronic structures. Thus the use of the ultrasoft pseudopotentials has a great advantage. The plane-wave cutoff E_{cut} was chosen to be 380 eV in the present study. This was confirmed to achieve a good convergence with respect to the total energy E_t ; the difference in the absolute value of the total energies by two calculations using $E_{\text{cut}}=380$ and 800 eV were 0.02, -0.03 , and -0.07 eV for H₂, LaNi₅, and LaNi₅H₇, respectively. When E_t of a compound with different atomic arrangements were compared, the relative value of the total energies ΔE was found to be converged within an accuracy of 0.01 eV LaNi₅H_{*x*} up to $E_{\text{cut}}=800$ eV. The convergence of the heat of formation as defined by Eq. (2), ΔH , was smaller than 0.02 eV/LaNi₅H₇.

It is well established that LaNi₅ exhibits a hexagonal structure with a space group of $P6/mmm$ (a structure type CaCu₅).²⁵ Its primitive cell is composed of a formula unit, i.e., $Z=1$. La atoms are located at the 1*a* site in the Wyckoff's notation. There are two Ni sites, i.e., 3*g* and 2*c*. The Brillouin-zone (BZ) sampling for LaNi₅ was performed using 75 **k** points in the whole first BZ. Calculation of the H₂ molecule was made using a supercell of $10 \times 10 \times 10 \text{ \AA}^3$ containing only one H₂ molecule. Its total energy was only 0.04 eV/H₂ less negative than that of H₂ molecular crystals calculated by the same method.

Calculations of hydrides were made by optimizing all degrees of freedom including cell parameters and internal coordinates within a given space group. The sizes of the unit cell for the calculation were $Z=1$ or 2. When we need to compare E_t at the same composition but different in Z , we have chosen a doubled cell for $Z=1$. However, the use of the doubled cell did not change the E_t per LaNi₅H_{*x*}. The error was always smaller than 0.01 eV. The density of **k** points in the whole first BZ was fixed to be approximately the same as that of the calculation of LaNi₅, i.e., at $6 \times 10^3 \text{ \AA}^3$. Convergence of E_t with respect to the number of **k** points was better than 0.01 eV/LaNi₅H_{*x*} with $x=0$ and 7. All calculations in the present study were made without taking the spin polarization into account. The total energy by the spin-polarized calculation was found to be smaller than the computational accuracy for LaNi₅H_{*x*} with $x=0, 0.5, 3$, and 7. The difference is in quantitative agreement with those reported by the theoretical calculation in Ref. 16. No quantum-nuclear ef-

fects for hydrogen were taken into account. We ignore the entropy terms throughout the present study when we compare the present results with experimental data. They remain challenging problems on the first-principles calculations.

III. RESULTS AND DISCUSSION

A. Structure of LaNi₅H₇

The structure of a full hydride has been repeatedly examined by means of neutron diffraction using deuterated samples. In early days a full hydride was described as LaNi₅H₆ having a space group of $P31m$ as summarized in Ref. 26. A careful Rietveld profile analysis by Lartigue, Le Bail, and Percheron-Guegan⁴ found that a LaNi₅D_{6,7} specimen can be described by a doubled unit cell of LaNi₅ along the *c* axis. Satisfactory refinement of the experimental profile was obtained in the space group $P6_3mc$ and also in the space group of $P31c$. The difference in the two space groups is due to the presence of a mirror plane leading to the atomic position of the 6*c* site to be (*x*, $-x$, *z*) in $P6_3mc$ instead of (*x*, *y*, *z*) in $P31c$. Due to the presence of the mirror plane, the atomic positions in two models are different. However, both models provided indistinguishable reliability factors within the experimental accuracy. We will hereafter call these two sets of atomic positions, suggested by Lartigue, Le Bail, and Percheron-Guegan, to be Model 1 and Model 2. Further refinement of the structure was made using anisotropic temperature factors only for the space group of $P6_3mc$. We adopted the set of atomic positions using the anisotropic temperature factors for Model 1.

Both the models can be described using five different *D* (deuteron) sites: two kinds of interstices of formal Ni₄ tetrahedrons (*D1* and *D2* in Ref. 4), two kinds of interstices of formal La₂Ni₂ tetrahedrons (*D3* and *D4* in Ref. 4), and one interstice of formal La₂Ni₄ octahedron (*D5* in Ref. 4). In the present study we use different notations in order to avoid confusion associated with the use of the same notations for different sites by different authors. *D1* and *D2* in Ref. 4 will be called *t*₁ and *t*'₁ sites. Their *D3* and *D4* will be called *t*₂ and *t*'₂ and *D5* will be *o* site. In this way, all the sites can be labeled by their local coordination, i.e., *t* for tetrahedral and *o* for octahedral. Two kinds of sites having the same local coordination are denoted by the same subscript, i.e., 1 or 2. According to the analysis reported in Ref. 4, the occupancy factors of both *t*'₁ and *t*'₂ sites are small. Sites with a prime mark, i.e., *t*'₁ and *t*'₂, correspond to the minority sites. In the Wyckoff's notation these sites are labeled differently depending upon the choice of the space group. The new notation should, therefore, be more useful and informative. These positions are shown in Fig. 1. *o* sites are located close to the $z=0$ of the host LaNi₅ cell, while *t*₁ and *t*₂ sites are located close to the $z=\frac{1}{2}$ of the host LaNi₅ cell.

Since the occupancy factors of both *t*'₁ and *t*'₂ sites are reported to be small,⁴ we will consider a model with the hypothetically ordered LaNi₅H₇ structure for the full hydride. *t*₁, *t*₂, and *o* sites are occupied by 2, 6, and 6 H atoms per La₂Ni₁₀H₁₄. Using the Wyckoff's notation, *t*₁, *t*₂, and *o* sites correspond to 2*b*, 6*c*, and 6*c* sites in the space groups of

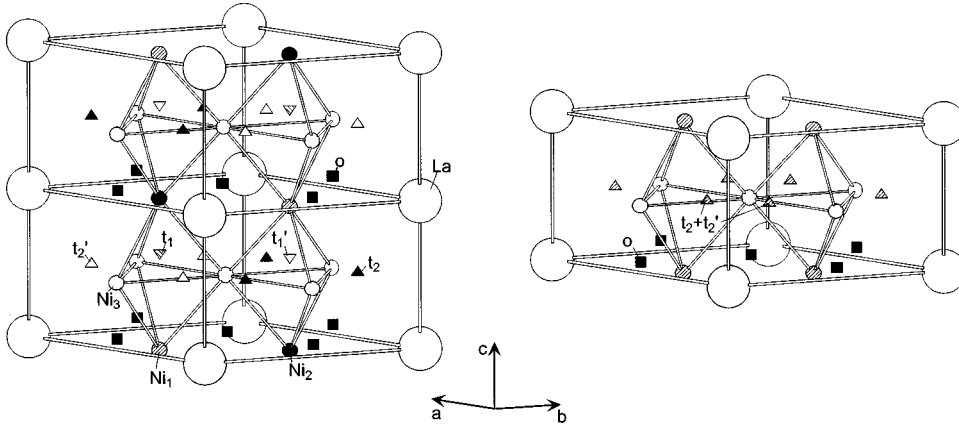


FIG. 1. Crystal structures of LaNi_5H_6 and LaNi_5H_7 . Left: The structure reported by Lartigue, Le Bail, and Percheron-Guegan (Ref. 4) with five different H sites and a double unit cell ($Z=2$). Right: The structure reported by Fisher *et al.* (Ref. 27) with two different H sites and a single unit cell ($Z=1$). Triangles denote the t_1 , t_2 , t_1' , and t_2' sites. Squares denote the o site. Large and small circles denote La and Ni atoms, respectively.

$P6_3mc$ and $P31c$. When t_1 , t_2 , and o sites are fully occupied, there is no ambiguity for the choice of the H-sites in the hypothetically ordered LaNi_5H_7 structure.

First, we adopt Model 1 and Model 2 within the hypothetically ordered structure to calculate the total energies and residual forces by the Hellmann-Feynman theorem. The results are shown in Table I. Model 1 gives total energy 0.34 eV/LaNi_5 unit lower than Model 2. At the same time, the maximum residual force is 2.12 eV/\AA in Model 2 and 0.46 eV/\AA in Model 1. These results clearly imply that Model 2 is less favorable, although the reliability factor by the experiment was good enough. It should be noted, however, that the maximum residual force is not negligible even in Model 1. Several reasons for the non-negligible residual force can be raised:

- (1) The experiments were done not on LaNi_5H_7 , but on $\text{LaNi}_5\text{D}_{6.7}$. The difference in D and H as well as the difference in the amount of D/H may not be neglected.
- (2) We use a model with a hypothetically ordered LaNi_5H_7 structure having full occupancy of t_1 , t_2 , and o sites, which is different from the real experimental results showing small occupancy of t_1' and t_2' sites.
- (3) Systematic errors on the equilibrium lattice volume due to the use of GGA. In order to find out optimized structures within the present theoretical framework, we made further calculations.

A full geometry optimization of LaNi_5H_7 was made imposing only space groups to be $P6_3mc$ and $P31c$. The de-

gree of freedom including cell parameters is 12 and 15 for $P6_3mc$ and $P31c$, respectively. Model 1 and Model 2 were taken to be the initial structures for calculations of $P6_3mc$ and $P31c$, respectively. The optimized structures obtained in this way will be called Model 1* and Model 2*. The asterisk will hereafter indicate the optimized structure. The optimization was truncated when the residual maximum force became smaller than $5 \times 10^{-2} \text{ eV/\AA}$. The optimized parameters for two models are listed in Table II together with experimental values. The cell parameters of Model 1* and Model 2* are different only slightly, which is in good agreement with the experimental values within errors of 0.5%. It is very interesting that internal parameters of Model 1* and Model 2* are very close to each other. The deviation in the internal parameters, Ξ^2 , as defined by Eq. (1) is as small as 1.5×10^{-4} :

$$\Xi^2 = \sum_n \sum_i (\xi_{A,n,i} - \xi_{B,n,i})^2, \quad (1)$$

where $\xi_{X,n,i}$ denotes the internal parameter of i th coordinate for n th atom in the Model X. It should also be emphasized that the theoretical internal parameters of Model 1* agree well with the experimental values in Model 1 ($\Xi^2 = 2.6 \times 10^{-4}$). The agreement is worse with Model 2 ($\Xi^2 = 2.2 \times 10^{-3}$). This means that the geometry optimization using both Model 1 and Model 2 as initial structures converged to almost the same structure, despite the imposition of different space groups. The internal parameters of Model 1* and

TABLE I. Theoretical results for six models of LaNi_5H_7 . ΔE_i shows the total energy relative to that of Model 1*.

Imposed space group	Total energy (eV/ LaNi_5H_7)	ΔE_i (eV/ LaNi_5H_7)	Maximum residual force (eV/ \AA)
Reported by experiments			
Model 1 $P6_3mc$	-6266.37	+0.07	0.46
Model 2 $P31c$	-6266.04	+0.41	2.12
Optimized in the present study			
Model 1* $P6_3mc$	-6266.44	0	<0.05
Model 2* $P31c$	-6266.45	-0.01	<0.05
Model 3* Cm^a	-6266.26	+0.18	<0.05
Model 4* $P3$	-6266.44	0.00	<0.05

^aHexagonal unit cell is imposed.

TABLE II. Cell parameters, a , c in Å and internal parameters of LaNi_5H_7 by four models.

$P6_3mc$ theory (Model 1*)			$P6_3mc$ experiment (Model 1)		
	a	c	a	c	
	5.384	8.621	5.409	8.600	
	x	y	x	y	z
La	0	0	0	0	0.022
Ni ₁	0.502	$-x$	0.498	$-x$	0.250
Ni ₂	$\frac{1}{3}$	$\frac{2}{3}$	$\frac{1}{3}$	$\frac{2}{3}$	0.002
Ni ₃	$\frac{1}{3}$	$\frac{2}{3}$	$\frac{1}{3}$	$\frac{2}{3}$	0.489
H(o)	0.506	$-x$	0.504	$-x$	0.056
H(t_1)	$\frac{1}{3}$	$\frac{2}{3}$	$\frac{1}{3}$	$\frac{2}{3}$	0.814
H(t_2)	0.161	$-x$	0.160	$-x$	0.280
$P31c$ theory (Model 2*)			$P31c$ experiment (Model 2)		
	5.379	8.622	5.409	8.600	
La	0	0	0	0	0.004
Ni ₁	0.501	-0.502	0.517	-0.486	0.250
Ni ₂	$\frac{1}{3}$	$\frac{2}{3}$	$\frac{1}{3}$	$\frac{2}{3}$	0.006
Ni ₃	$\frac{1}{3}$	$\frac{2}{3}$	$\frac{1}{3}$	$\frac{2}{3}$	0.497
H(o)	0.506	-0.507	0.510	-0.490	0.057
H(t_1)	$\frac{1}{3}$	$\frac{2}{3}$	$\frac{1}{3}$	$\frac{2}{3}$	0.830
H(t_2)	0.158	-0.158	0.154	-0.168	0.299

Model 2* being very close to those of model 1, the set of internal parameters used in Model 1 should be a better choice than those used in Model 2. This is consistent with the above-mentioned result obtained for Model 1 and Model 2 on the basis of energies and residual forces. We can, therefore, conclude that Model 2 is an artifact at the Rietveld analysis.

It is difficult to discuss the preference of the $(11\bar{2}0)$ mirror plane to make the space group to be $P6_3mc$ from the $P31c$ structure because of the small energy difference. According to the present calculation, Model 2* with the space group of $P31c$ is lower in energy by 0.01eV/ LaNi_5H_7 than Model 1* with the space group of $P6_3mc$, although atomic positions in both models are very close to each other. However, the difference in energy is close to the accuracy of the present calculation. We have investigated two more hypothetical LaNi_5H_7 to examine their stabilities.

Before the work by Lartigue, Le Bail, and Percheron-Guegan,⁴ the structure of full hydride was described as having a primitive cell with $Z=1$. Fischer *et al.*²⁷ described a LaNi_5D_6 compound with H atoms fully occupying the $3c$ site ($D1$ in Ref. 27), and partially occupying the $6d$ site ($D2$ in Ref. 27) of the $P31m$ structure. The $3c$ site corresponds to the o site in Fig. 1. On the other hand, the $6d$ site includes not only the t_2 site but also the t'_2 site. In the space group of $P31m$, t_2 and t'_2 are equivalent. We extrapolate the model by Fischer *et al.* to LaNi_5H_7 , with three H at o site and four at $t_2+t'_2$ sites, which will be called Model 3. The distribution of H in this model is different from Models 1 and 2 having three H at o site, three at t_2 site, and one at t_1 site.

The total energy of the optimized structure of Model 3,

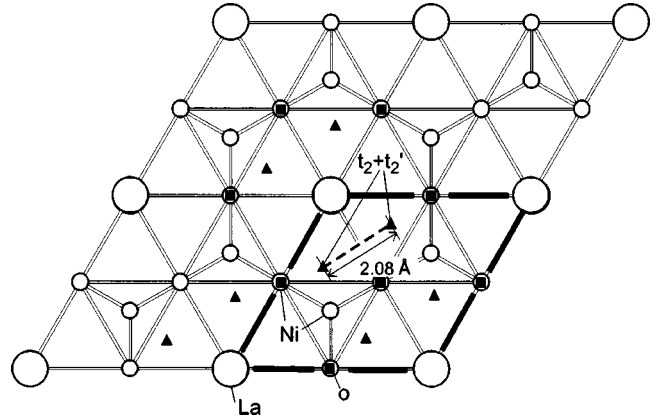


FIG. 2. The array of atoms projected on the (0001) plane for Model 3* of LaNi_5H_7 . The thick lines make a unit cell.

i.e., Model 3*, is 0.18 eV/ LaNi_5H_7 greater than that of Model 1* as shown in Table I. The occupation of four H at $t_2+t'_2$ sites is clearly unfavorable. The atomic positions of Model 3* are displayed in Fig. 2. The H atoms at $t_2+t'_2$ sites moved to avoid each other. Nevertheless, the distance between H atoms at the nearest neighbor $t_2+t'_2$ sites is 2.08 Å, which is 25% smaller than the nearest-neighbor bond length of H atoms between t_2 sites in Model 1* i.e., 2.60 Å. Westlake²⁸ investigated atomic positions of metal hydrides systematically and found an empirical rule for stable hydrogen sites. According to the criterion, stable hydrogen should have nearest-neighbor H-H distance of greater than 2.1 Å. The higher energy of Model 3* is consistent with the criterion, since the shortest H-H distance in Model 3*, 2.08 Å, is smaller than the critical value 2.10 Å. The $t_2+t'_2$ sites can, therefore, accommodate only three H per LaNi_5 at most.

If the occupancy of three H at o site, three at t_2 site, and one at t_1 site is the only major requirement for the stable LaNi_5H_7 structure, a model with another space group having a single-unit cell may not be energetically unfavorable too much. In order to confirm the idea, we made a model of LaNi_5H_7 (Model 4*) with a single-unit cell and three H at o site, three at t_2 , and one at t_1 . Geometry optimization was made only by imposing $P3$ symmetry. The energy of Model 4* is found to be indistinguishable to that of Model 1*. The structure model with a single-unit cell, i.e., $Z=1$, cannot be ruled out by the theoretical calculation on the hypothetically ordered LaNi_5H_7 .

B. Remarks on the structure of LaNi_5H_6

In the preceding section, we found that the occupancy of four H at $t_2+t'_2$ sites is energetically unfavorable for LaNi_5H_7 . The occupancy of three H at o , three at t_2 , and one at t_1 site is the major requirement to have a stable LaNi_5H_7 structure. Since the full hydride has been described as LaNi_5H_y ($6 \leq y < 7$), it is interesting to examine the preference of sites between t_1 and t_2 in LaNi_5H_6 . In order to evaluate the difference, two models for LaNi_5H_6 with $Z=1$ were first employed: One contains three H at o and three at t_2 sites. The other has three H at o , one at t_1 , and two at t_2 sites. Total energies after geometry optimization are com-

TABLE III. Theoretical results for four models of LaNi_5H_6 . ΔE_t shows the total energy relative to that of the lowest one.

	Number of H atoms (atoms/ LaNi_5H_6)			Imposed space group	Total energy (eV/ LaNi_5H_6)	ΔE_t (eV/ LaNi_5H_6)
	t_1	t_2	o			
Z=1 (single unit cell)						
LaNi_5H_6 #1	0	3	3	$P3$	-6250.18	0
LaNi_5H_6 #2	1	2	3	Cm^a	-6250.16	+0.02
Z=2 (double unit cell)						
$\text{LaNi}_{10}\text{H}_{12}$ #1	0	3	3	$P6_3mc$	-6250.15	+0.03
$\text{LaNi}_{10}\text{H}_{12}$ #2	1	2	3	$Cmc2_1^a$	-6250.14	+0.03

^aHexagonal unit cell is imposed.

pared in Table III. The former model (#1) is energetically favorable by 0.02 eV/ LaNi_5H_6 . Although the difference in energy is small, the t_2 site is slightly preferred than the t_1 site in LaNi_5H_6 . As referred to in the preceding section, Fischer *et al.*²⁷ described a LaNi_5H_6 crystal with a primitive cell of $Z=1$ and three H at o sites and three H at t_2+t_2' sites. The present result suggests that the model by Fischer *et al.* can work for LaNi_5H_6 , although it cannot be used for LaNi_5H_7 because of the ignorance of the t_1 site.

In the preceding section the total energy of the cell with $Z=1$ is found to be very close to that with $Z=2$ for LaNi_5H_7 . As for LaNi_5H_6 , the total energy with $Z=1$ is found to be smaller than that with $Z=2$ by 0.03 eV/ LaNi_5 when model 1 is used as shown in Table III. When the model #2 is used, the same trend can be seen though the energy difference is smaller. Regarding the LaNi_5H_6 , there is no reason to have a $Z=2$ cell if the structure is restricted to the hypothetically ordered structure as employed in the present study.

C. Structure of primary solid solution

Five nonequivalent interstices have been argued as possible hydrogen sites in the primary solid solution of $\text{LaNi}_5\text{-H}$ within the space group of $P6/mmm$. A number of experimental neutron-diffraction studies have been reported. Gray *et al.*²⁹ made a review of experimental works. The $3f$ and/or $12n$ sites have been most frequently concluded as the preferred occupation sites.^{27,30,31} On the other hand, Hempelmann *et al.*³² reported that both $3f$ and $6m$ were occupied. First-principles calculations by Nakamura, Nguyen-Manh, and Pettifor¹⁵ concluded that $6m$ was the preferred occupation site. However, they have used a simplified model derived from a rigid-sphere model in Ref. 30, and they did not optimize the structure.

Stable hydrogen sites have often been argued using the rigid-sphere model for atomic structure. The size of atomic holes has been computed to discuss the experimental results. Westlake²⁸ proposed that the minimum hole size is 0.4 Å to stabilize the hydrogen atoms at interstices. Soubeyroux, Percheron-Guegan, and Achard³⁰ made a rigid-sphere model on the basis of their experimental results and discussed the relative stability of hydrogen atoms at different interstices.

However, the rigid-sphere model is certainly an overly simplified model in general. Its validity or limitation should be examined by other methods.

In the present study, we made three sets of calculations. In the first set, #1, the cell parameters were fixed at the theoretical values of LaNi_5 that were optimized in the present study. Internal parameters were fixed at values shown in Ref. 30 by a rigid-sphere model. In the second set, #2, the cell parameters were fixed to be the same as in #1. Only internal parameters were optimized. In the third set, #3, all parameters including the cell constants were optimized imposing a hexagonal lattice. Calculations were made for a double cell of LaNi_5 with one H at a specific site, i.e., $\text{La}_2\text{Ni}_{10}\text{H}_1$. The cell was chosen because the solubility limit of H in the primary solid solution has been reported to be close to $x=0.5$, (Refs. 33 and 34) in the formula of LaNi_5H_x . The present calculation roughly corresponds to the composition at the solubility limit. All calculations were made under possible-highest symmetry when one H is present. In other words, geometry optimization was made imposing the space group made by the original $\text{La}_2\text{Ni}_{10}$ cell and one H at the specific site. These calculations were made in order to compare the stability of H at five different sites. With the imposition of the symmetry, higher energy sites can be calculated. Otherwise, higher energy structure may disappear during the geometry optimization.

The theoretical heats of solution by the present calculations are listed in Table IV. By the calculations #1 without any geometry optimization, all interstices show positive values of the heat of formation (solution). The value is lowest for $12n$ and second lowest for $6m$. It is interesting to note that these two sites were reported to have the hole radius greater than 0.4 Å. If we restrict ourselves to the unrelaxed geometry, the Westlake's criteria²⁸ seem to work qualitatively. Nakamura, Nguyen-Manh, and Pettifor¹⁵ made a similar calculation without relaxation and reported that all of their heats of formation were having positive values. Contrary to the present work, however, the $12n$ site showed much higher energy in their work.

When the geometry is optimized, the relative stability of H changes dramatically. Relaxation energy can be defined by the difference in energies between #1 and #3. It is largest for the $4h$ site, and smallest for the $6m$ site. As a result, $6m$

TABLE IV. Theoretical energy of formation (solution) of H (eV/La₂Ni₁₀H₁) at five interstices using the model of the solid solution, i.e., La₂Ni₁₀H₁.

Occupied site	#1	#2	#3
12 <i>n</i>	0.10	-0.14	-0.17
3 <i>f</i>	0.19	-0.09	-0.12
12 <i>o</i>	0.28	-0.02	-0.07
6 <i>m</i>	0.12	0.01	-0.02
4 <i>h</i>	0.24	-0.08	-0.14

became the highest energy site. Although the cell volume increased by 2–3 % in the #3 calculations as compared with the #2, both sets of the calculations, #2 and #3 show a similar trend. Eventually there is no clear correlation between the initial hole radius and the stability in the optimized structures.

In order to find out the presence of a more stable position of H another calculation was made without imposing any specific symmetry operations except for the hexagonal lattice. H was put at a position not exactly but close to the 12*n* site in the initial structure. After the geometry optimization we found that the H atom was located at a position that is indistinguishable from the 12*n* site optimized by set 3 calculation. We can therefore conclude that the 12*n* site is the most stable position in the hexagonal La₂Ni₁₀H₁ lattice. Geometry of the optimized La₂Ni₁₀H₁ lattice is summarized in Table V.

In order to understand the mechanism to determine the relative stability among the H sites, we have analyzed the local environment of the H atoms after the geometry optimization, i.e., #3 structures. Radial distribution of atoms is plotted in Fig. 3. As can be seen, the local coordination is not so simple to distinguish the first shell from the second in general. Among them the 3*f* site is relatively simple. The H atom at the 3*f* site is coordinated by 6 atoms (4 Ni and 2 La) within the bond-length of 2.6 Å. It is then coordinated by eight Ni atoms with the bond length of 3.2 Å. The situation is similar to the octahedral interstice of the face-centered cubic (fcc) lattice. The shortest distance between the interstices of the optimized structure (#3) is summarized in Table VI. The

TABLE V. Theoretical structure of the La₂Ni₁₀H₁ model having H at the 12*n* site (#3 calculation).

Imposed symmetry	<i>a</i> (Å)		<i>c</i> (Å)
<i>Cm</i> ^a	5.075		7.866
	<i>x</i>	<i>y</i>	<i>z</i>
La ₁	-0.001	<i>x</i>	-0.009
La ₂	-0.001	<i>x</i>	0.499
Ni ₁	0.497	<i>x</i>	0.247
Ni ₂	0.497	<i>x</i>	0.751
Ni ₂	-0.003	0.497	0.245
Ni ₃	0.662	0.333	0.000
Ni ₄	0.676	0.315	0.503
Ni ₅	0.662	0.333	0.000
H(12 <i>n</i>)	0.496	<i>x</i>	0.456

^aHexagonal unit cell is imposed.

12*n* site after the geometry optimization is located only 0.35 Å away from the 3*f* site and it has similar local environment as the 3*f* site. This is inconsistent with the rigid-sphere model claiming that the 12*n* site is a tetrahedral site.³⁰ It is interesting that the radial distribution around the 12*n* site is close to that of the *o* site in the full hydride as shown in Fig. 3. The 12*n* site should be described as an octahedral interstitial site that is located slightly off center.

The 4*h* site is another simple site. It is basically coordinated by four Ni atoms at 1.6 Å, which are followed by one Ni atom at 2.4 Å. This is analogous to the *t*₁ site in the full hydride. On the other hand, local structures of 12*o* and 6*m* are more complicated than the others. According to the rigid-sphere model, both are tetrahedral sites coordinated by 3 Ni+1 La and 2 Ni+2 La, respectively. Although the feature is somehow maintained after the geometry optimization, the first shell is hardly distinguishable from the second. Correspondence between these sites and the *t*₂ site is less clear than the other sites, either.

As shown in Table IV, the 12*n* site is energetically more favorable than the 3*f* site by 0.05 eV. It seems the deviation of H from the 3*f* to the off-center 12*n* position is driven by the increase in the number of short Ni-H bonds. We can further hypothesize that the number of Ni-H bonds at the near neighbor is an important parameter to determine the stability. The idea qualitatively explains the general trend of the stability. Table VII summarizes the near-neighbor bond length and the number of bonds. The number of Ni atoms within 1.8 Å is 3, 4, 4, 3, and 2 for 12*n*, 4*h*, 3*f*, 12*o*, and 6*m*, respectively. The energy of solution increases with the decrease in the number of the near-neighbor Ni atoms, except for the case of 12*n*. We cannot find such a correlation when we adopt the number of near neighbor La atoms. Of course, the hypothesis is too simple to be used quantitatively. We have to take into account other bonds, such as, Ni-Ni for precise discussion. But at least the idea provides the physical insight as to how the order of the stability is determined in this way. Yukawa, Matsumura, and Morinaga¹⁴ made a series of cluster calculations to investigate chemical bonding in metal hydrides. According to them, the La-H bonds are much weaker than the Ni-H bonds as evaluated by bond-overlap populations. This is consistent with our hypothesis given in this work. Then a question can be raised: why the pure Ni does not have enough solubility of H? Experiments show that the heat of solution of H in fcc Ni is a positive value, i.e., +32 kJ/mol-H₂.³⁵ The answer can be suggested by revisiting the #1 calculation of the primary solid solution. In the unrelaxed structure, although the 4*h* site has the largest coordination number of Ni, it exhibits positive energy of solution. The 4*h* site can be stabilized significantly only when the near-neighbor Ni atoms are allowed to relax. The presence of La having large atomic size may make the room for the relaxation. This should be one of the major roles of La to make LaNi₅ to be a superior hydrogen storage material. In a closed-packed lattice, such as in fcc Ni, such significant relaxation may not be allowed, which can be the reason for the positive heat of solution. As a matter of fact, the atomic density of LaNi₅ is 6.9×10^{-2} atom/Å³, which is 25% less dense than that of fcc Ni, 9.2×10^{-2} atom/Å³. CaNi₅ is iso-

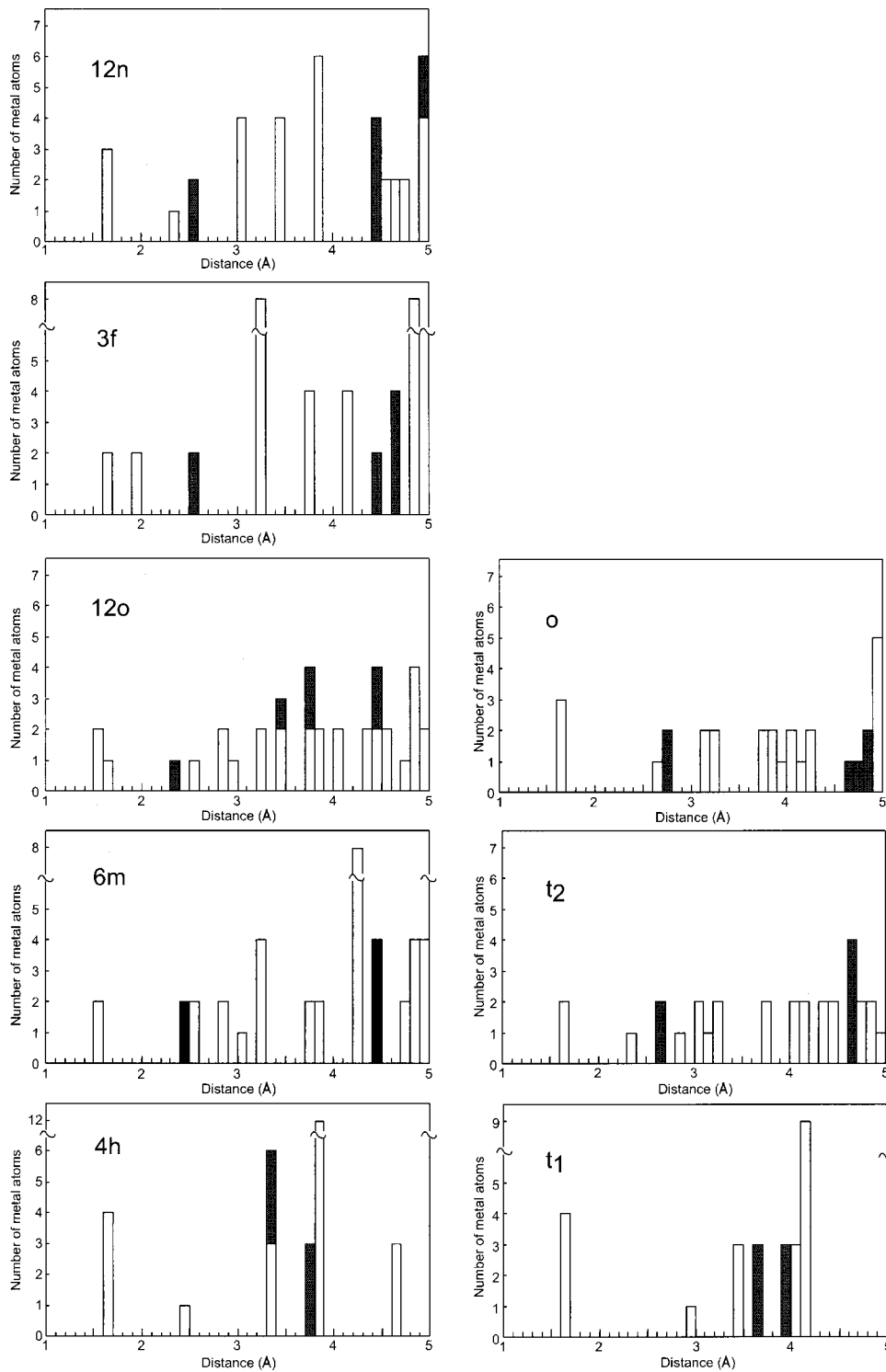


FIG. 3. Radial distribution of near-neighbor La or Ni atoms around a H atom at the interstice. Left: The models for primary solid solutions, $\text{LaNi}_5\text{H}_{0.5}$. Right: The model for LaNi_5H_7 (Model 1*).

structural to LaNi_5 , having an atomic density of $7.1 \times 10^{-2} \text{ atom}/\text{\AA}^3$, shows good hydrogen storage capability, too.

D. Heat of formation of hydrides and heat of solution of H in LaNi_5

The theoretical heat of formation of LaNi_5H_7 relative to LaNi_5 and H_2 can be calculated by the following equation:

$$\Delta H = E_t[\text{LaNi}_5\text{H}_7] - (E_t[\text{LaNi}_5] + 7/2E_t[\text{H}_2]), \quad (2)$$

where E_t is the total energy calculated for the unit formula shown in the parenthesis. ΔH is obtained to be $-1.63 \text{ eV}/\text{LaNi}_5\text{H}_7$, or $-44.9 \text{ kJ}/\text{mol-H}_2$. This is 30–40% more negative than the experimental heat of formation of the full hydride in literature ranging from -32 to $-35 \text{ kJ}/\text{mol-H}_2$.^{33,36} This discrepancy may be ascribed to the fact that hydride samples are generally highly defective. For

TABLE VI. Shortest distances between interstices in Å in #3 calculation.

	12n	3f	12o	6m	4h
12n		0.35	1.52	2.22	1.91
3f			1.73	2.48	2.15
12o				1.01	1.06
6m					1.64
4h					

example, high density of dislocations of the order of 10^{15} m^{-2} are generally present in the full hydride samples.⁵⁻⁸ Positron-annihilation study by Shirai *et al.* detected high concentration of vacancies in the hydride samples.⁹ Energies associated with the crystalline defects may have non-negligible effects on the experimental heat of formation.

The theoretical work by Nakamura, Nguyen-Manh, and Pettifor¹⁵ used the unrelaxed Model 1 to obtain the heat of formation of -57.3 kJ/mol-H_2 . Their result is far more negative than the present result for the same model, i.e., -42.9 kJ/mol-H_2 . The discrepancy between two theoretical results may be ascribed to the difference in computational techniques.

The heat of solution obtained for the 12n site by #3 calculation of $\text{La}_2\text{Ni}_{10}\text{H}_1$ is -32.8 kJ/mol-H_2 . Experimental enthalpy in the primary solid solution has been reported as a function of the H concentration by several groups,^{33,36,37} which agree to each other. It is $< -50 \text{ kJ/mol-H}_x$ in the region of $x < 0.05$ of LaNi_5H_x . It became less negative with the increase of x . It shows the lowest negative value of -26.5 or -28 kJ/mol-H_2 near solubility limit of the primary solid solution. The former value has been ascribed to the energy for hydrogen chemisorption and/or trapping. The latter value has been accepted as the real heat of solution of H in LaNi_5 solid solution. In the low- x region, the computational error is larger when converted to the unit of $\text{kJ mol}^{-1}\text{H}_2$ as compared to the errors for hydrides. The error of $\pm 0.01 \text{ eV/LaNi}_5\text{H}_{0.5}$ corresponds to $\pm 3.9 \text{ kJ/mol-H}_2$. Taking computational error in consideration, the present theoretical value is in rough agreement with the experimental one. A slightly more negative value may be ascribed to the high density of crystalline defects similar to the case of the full hydride, because the calorimetric measurements have been made on samples after repeated hydrogenation cycles.

In the $\text{LaNi}_5\text{-H}$ system, an intermediate phase between the primary solid solution and the full hydride has been reported.³⁸⁻⁴¹ Its composition is close to LaNi_5H_3 , which

TABLE VII. Averaged bond length between H and neighboring metal atoms, d , and number of bonds, N . Metal atoms within $d_{\text{H-Ni}} < 1.8 \text{ \AA}$ and $d_{\text{H-La}} < 3.0 \text{ \AA}$ were adopted.

	$d_{\text{H-Ni}}$	$N_{\text{H-Ni}}$	$d_{\text{H-La}}$	$N_{\text{H-La}}$
12n	1.64	3	2.56	2
3f	1.71	4	2.54	2
12o	1.59	3	2.33	1
6m	1.57	2	2.42	2
4h	1.61	4		

TABLE VIII. Theoretical results for two models of LaNi_5H_3 . ΔH shows the theoretical energy of formation.

	Hydrogen sites	Total energy (eV/ LaNi_5H_3)	ΔH (eV/ LaNi_5H_3)
Model A	3(<i>o</i>)	-6201.44	-0.49
Model B	2(<i>o</i>) + 1(<i>t</i> ₂)	-6201.44	-0.50

was reported to be stable at above 353 K. It may be interesting to investigate the heat of formation of LaNi_5H_3 in order to know whether the phase is a stable one. Akiba *et al.*⁴² described the structure of LaNi_5H_3 with the space group $P6/mmm$ that is the same as that of LaNi_5 . Since site occupancies of H cannot be determined uniquely in LaNi_5H_3 , several sets of calculations were made in the present study. There are two kinds of H sites in the model by Akiba *et al.*, i.e., 6*i* and 6*m* sites of the space group of $P6/mmm$ ($Z=1$). They are, respectively, analogous to *o* and *t*₂ sites of the full hydrides. We have selected three H sites among 6*i* + 6*m* sites to put H atoms, and made calculations systematically. Two lowest-energy configurations were then found after full geometry optimization using a hexagonal primitive cell of LaNi_5H_3 ($Z=1$) imposing the space group made by the original LaNi_5 cell and three H at the given sites. The first model has three H at the *o* site (Model A). The second model has two H at the *o* site and one at the *t*₂ site (Model B). The energies of these two models are almost the same as shown in Table VIII.

In order to examine the energetics of the low- x region, we made an extra calculation at $x=1$. Calculation was made using a model with one H at the 12n position and a $Z=1$ cell. Geometry was fully optimized to obtain the heat of formation (solution). It is interesting to compare the theoretical heat of formation of hydrides at various compositions.

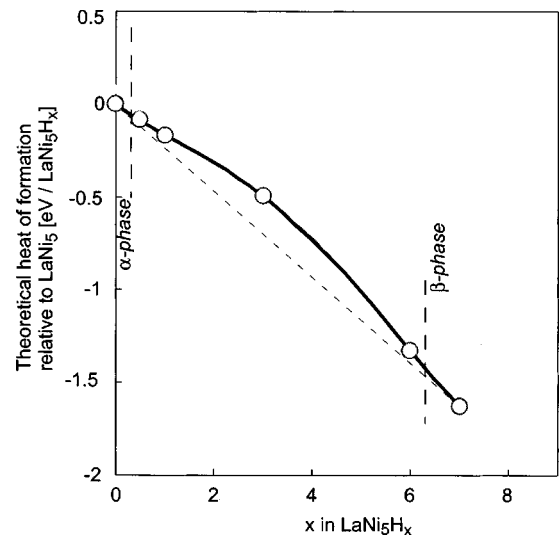


FIG. 4. Theoretical heat of formation of six models as a function of H content, x , relative to the energy of LaNi_5 . The phase boundaries correspond to averaged experimental values in many reports. Note that they were not determined by the calculation.

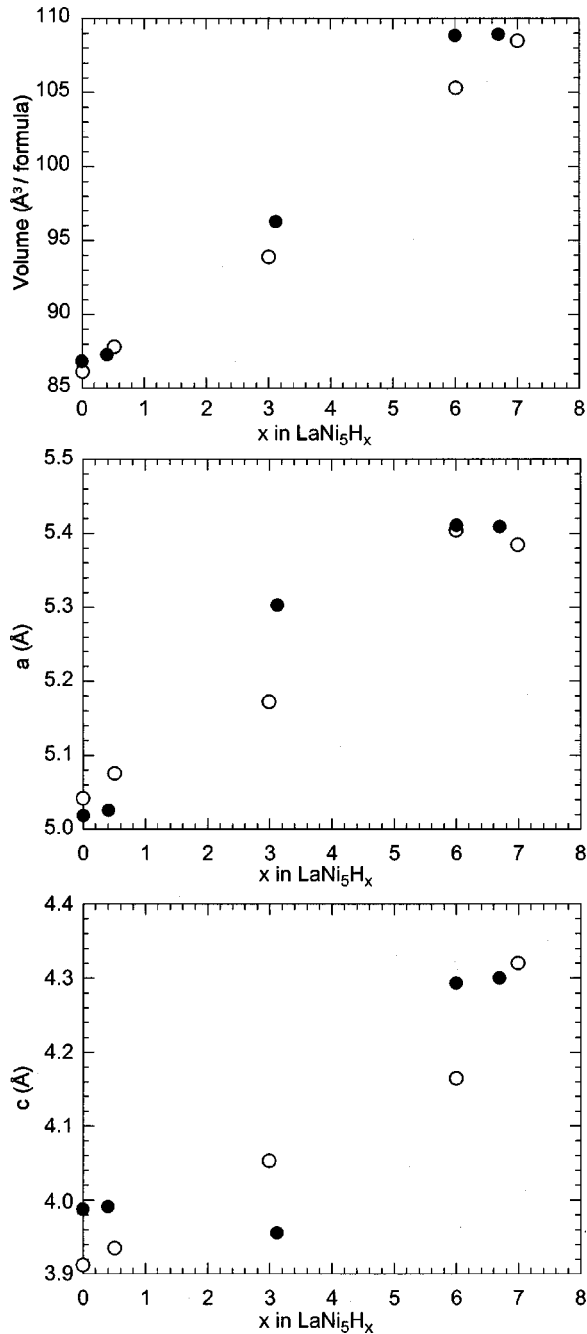


FIG. 5. Comparison of (top) volume, lattice constants (middle) a and (bottom) c between calculated (open circles) and experimental (closed circles) (Refs. 4,27,30,42) for composition, x .

The heat of formation of LaNi_5H_1 , LaNi_5H_3 , and LaNi_5H_6 are plotted together with the values of $\text{LaNi}_5\text{H}_{0.5}$ and LaNi_5H_7 in Fig. 4. The figure clearly indicates that the $\text{LaNi}_5\text{-H}$ system dissociates to the primary solid solution (α phase) and the hypothetically ordered LaNi_5H_7 (β phase) in the range of the intermediate composition. Owing to computational limitation, it is not possible to determine the solubility limit of H in LaNi_5 . When we ignore the entropy contribution, it should be lower than $x=0.5$, if any. The solubility limit has not been determined precisely even by experiments. It has been reported to be in the range of $x=0.34$ and

0.42.^{33,34} The present result is consistent with the experimental solubility.

When the heat of formation of the primary solid solution and that of the full hydride is connected as shown in Fig. 4 using a broken line, the value of LaNi_5H_3 is 0.18 eV/ LaNi_5H_3 greater than the value on the line at the same composition. Although the LaNi_5H_3 is stable only at temperatures above 353 K,⁴¹ the energy of 0.18 eV may be too large to stabilize the phase at such a moderate temperature. Buckley, Gray, and Kisi⁴⁰ discussed that the microstructural modification associated with the ordering of dislocations is required to stabilize LaNi_5H_3 phase. This kind of mesoscopic mechanism should be taken into account in order to explain the experimental results.

E. Volume expansion in $\text{LaNi}_5\text{-H}$ system

Figure 5 summarizes the theoretical lattice volume and cell parameters together with experimental values. A volume expansion by 25% has been reported by experiment from LaNi_5 to the full hydride,^{4,27} which is very well reproduced by the present calculations. Some deviation in volume can be found at the intermediate compositions. The values may be less accurate both in experiments and calculations as compared with those of the end members. The disagreement in the intermediate compositions is more pronounced in cell parameters, a and c . Further investigation on the origin of errors may reveal detailed structural information of the intermediate phases. However, it is beyond the scope of the present study.

IV. CONCLUSIONS

First-principles calculations have been made on phases in the $\text{LaNi}_5\text{-H}$ system with full geometry optimization using ultrasoft pseudopotentials and plane-wave basis. Results can be summarized as follows.

(1) The atomic positions of the full hydride have been described in two ways through the Rietveld analyses of experimental profile. The lowest-energy structure by the present calculation is close to that of the model analyzed with the space group of $P6_3mc$ by Lartigue, Le Bail, and Percheron-Guegan.⁴ Structure with four H at $t_2+t'_2$ sites is found to be unfavorable, which can be explained by a tight H-H packing. The $t_2+t'_2$ sites can accommodate only three H per LaNi_5 at most. One H should therefore occupy t_1 site in LaNi_5H_7 . Three H at o site, three at t_2 site, and one at t_1 site is, therefore, the major requirement to have a stable LaNi_5H_7 structure. We found that the structure models with different space group including those with a single-unit cell, i.e., $Z=1$, cannot be ruled out by the theoretical calculation on the hypothetically ordered LaNi_5H_7 .

(2) The model by Fischer *et al.*²⁷ can work for LaNi_5H_6 , although it cannot be used for LaNi_5H_7 .

(3) The $12n$ site of the LaNi_5 is found to be most stable among five possible interstices in the model of the primary solid solution, i.e., $\text{La}_2\text{Ni}_{10}\text{H}_1$ model. The $12n$ site can be described as the off-center octahedral site rather than the tetrahedral site. The deviation from the center is driven by

the increase in the number of the short Ni-H bonds. The formation energy can be qualitatively explained by the number of near-neighbor Ni atoms. Good analogy can be found between the $12n/3f$ sites and the o site in the full hydride by the examination of radial distribution of coordinated atoms. Radial distribution around the $4h$ and the t_1 sites are similar, too. On the other hand, poor correspondence can be found between the $12o/6m$ and the t_2 site.

(4) Theoretical heat of solution using the $\text{La}_2\text{Ni}_{10}\text{H}_1$ model is -33 kJ/mol- H_2 , which roughly agrees with the experimental value. On the other hand, theoretical heat of formation of the LaNi_5H_7 is -45 kJ/mol- H_2 , which is 30–40% more negative than the experimental value. The discrepancy may be ascribed to the fact that hydride samples are full of crystalline defects.

(5) Theoretical heat of formation of intermediate phases indicates that the $\text{LaNi}_5\text{-H}$ system dissociates to the primary solid solution (α phase) and the hypothetically ordered LaNi_5H_7 (β phase), which is consistent with the experimental results.

(6) Expansion of the cell volume associated with hydrogenation is well reproduced by the calculation.

ACKNOWLEDGMENTS

We would like to thank Dr. F. Oba for helpful discussions. This work was supported by the Grant-in-Aids for Scientific Research on Priority Areas (No. 751) from the Ministry of Education, Science, Sports, and Culture of Japan.

*Author to whom all correspondence should be addressed. Email address: kazu@cms.MTL.kyoto-u.ac.jp

¹J. J. G. Willems and K. H. J. Buschow, *J. Less-Common Met.* **129**, 13 (1987).

²J. H. N. van Vucht, F. A. Kuijpers, and H. C. A. M. Bruning, *Philips Res. Rep.* **25**, 133 (1970).

³*Hydrogen in Intermetallic Compounds I* edited by L. Schlapbach, Topics in Applied Physics Vol. 63 (Springer-Verlag, Berlin, 1988); *Hydrogen in Intermetallic Compounds II*, edited by L. Schlapbach, Topics in Applied Physics Vol. 67 (Springer-Verlag, Berlin, 1992).

⁴C. Lartigue, A. Le Bail, and A. Percheron-Guegan, *J. Less-Common Met.* **129**, 65 (1987).

⁵A. Percheron-Guegan, C. Lartigue, J.-C. Achard, P. Germi, and F. Tasset, *J. Less-Common Met.* **74**, 1 (1980).

⁶R. Cerny, J.-M. Joubert, M. Latroche, A. Percheron-Guegan, and K. Yvon, *J. Appl. Crystallogr.* **33**, 997 (2000).

⁷E. Wu, E. H. Kishi, E. Mac, and A. Gray, *J. Appl. Crystallogr.* **31**, 363 (1998).

⁸H. Inui, T. Yamamoto, M. Hirota and M. Yamaguchi, *J. Alloys Compd.* (to be published).

⁹Y. Shirai *et al.*, *J. Alloys Compd.* (to be published).

¹⁰H. Züchner, J. Kintrop, R. Dobrileit, and I. Untiedt, *J. Less-Common Met.* **293–295**, 202 (1999).

¹¹S. K. Malik, F. J. Arlinghaus, and W. E. Wallace, *Phys. Rev. B* **25**, 6488 (1982).

¹²M. Gupta, *J. Less-Common Met.* **130**, 219 (1987).

¹³T. Suenobu, I. Tanaka, H. Adachi, and G. Adachi, *J. Alloys Compd.* **221**, 200 (1995).

¹⁴H. Yukawa, T. Matsumura, and M. Morinaga, *J. Alloys Compd.* **293–295**, 227 (1999).

¹⁵H. Nakamura, D. Nguyen-Manh, and D. G. Pettifor, *J. Alloys Compd.* **281**, 81 (1998).

¹⁶M. Gupta, *J. Alloys Compd.* **307**, 290 (2000).

¹⁷A. Szajek, M. Jurczyk, and W. Rajewski, *J. Alloys Compd.* **307**, 290 (2000).

¹⁸J. P. Perdew, J. A. Chevary, S. H. Vosko, K. A. Jackson, M. R. Pederson, D. J. Singh, and C. Riola, *Phys. Rev. B* **46**, 6671 (1992).

¹⁹The present calculations were performed using the CASTEP program code (Molecular Simulations, Inc., San Diego, CA).

²⁰G. Kresse and J. Furthmüller, *Phys. Rev. B* **54**, 11 169 (1996).

²¹M. C. Payne, M. P. Teter, D. C. Allan, T. A. Arias, and J. D. Joannopoulos, *Rev. Mod. Phys.* **64**, 1045 (1992).

²²W. H. Press, S. A. Teukolsky, W. T. Vetterling, and B. P. Flannery, *Numerical Recipes*, 2nd ed. (Cambridge University Press, Cambridge, 1992), p. 418.

²³D. Vanderbilt, *Phys. Rev. B* **41**, 7892 (1990).

²⁴V. Milman, B. Winkler, J. A. White, C. J. Pickard, M. C. Payne, E. V. Akhmatkaya, and R. H. Nobes, *Int. J. Quantum Chem.* **77**, 895 (2000).

²⁵J. H. Wernick and S. Geller, *Acta Crystallogr.* **12**, 662 (1959).

²⁶D. G. Westlake, *J. Less-Common Met.* **91**, 275 (1983).

²⁷P. Fischer, A. Furrer, G. Busch, and L. Schlapbach, *Helv. Phys. Acta* **50**, 421 (1977).

²⁸D. G. Westlake, *J. Less-Common Met.* **90**, 251 (1983).

²⁹E. M. A. Gray, M. Kemali, J. Mayers, and J. Norland, *J. Alloys Compd.* **253–254**, 291 (1997).

³⁰J. L. Sobeyroux, A. Percheron-Guegan, and J. C. Achard, *J. Less-Common Met.* **129**, 181 (1987).

³¹E. H. Kisi, E. M. A. Gray, and S. J. Kennedy, *J. Alloys Compd.* **216**, 213 (1994).

³²R. Hempelmann, D. Richter, and G. Eckold, *J. Less-Common Met.* **104**, 1 (1984).

³³J. J. Murray, M. L. Post, and J. B. Taylor, *J. Less-Common Met.* **80**, 211 (1981).

³⁴E. H. Kisi, E. M. A. Gray, and S. J. Kennedy, *J. Alloys Compd.* **216**, 123 (1994).

³⁵K. Zeng, T. Klassen, W. Oelerich, and R. Bormann, *J. Alloys Compd.* **283**, 151 (1999).

³⁶W. N. Hubbard, P. L. Rawlins, P. A. Connick, R. E. Stedwell, Jr., and P. A. G. O'hare, *J. Chem. Thermodyn.* **15**, 785 (1983).

³⁷B. S. Bowerman, C. A. Wulff, and T. B. Flanagan, *Z. Phys. Chem., Neue Folge* **116**, 197 (1979).

³⁸S. Ono, K. Nomura, E. Akiba, and H. Uruno, *J. Less-Common Met.* **113**, 113 (1985).

³⁹K. Nomura, H. Uruno, S. Ono, H. Shinozuka, and S. Suda, *J. Less-Common Met.* **107**, 221 (1985).

⁴⁰C. E. Buckley, E. M. A. Gray, and E. H. Kisi, *J. Alloys Compd.* **231**, 460 (1995), and Refs. 7–14 therein.

⁴¹M. L. Post and J. J. Murray, *J. Solid State Chem.* **86**, 160 (1990).

⁴²E. Akiba, H. Hayakawa, Y. Ishido, K. Nomura, and S. Shin, *Z. Phys. Chem., Neue Folge* **163**, 291 (1989).